Dynamic mechanostereochemical switching of a co-conformationally flexible [2]catenane controlled by specific ionic guests

Yueliang Yao,[1] Yuen Cheong Tse,[1] Samuel Kin-Man Lai,[1] Yixiang Shi,[1] Kam-Hung Low[1] and Ho Yu Au-Yeung[1,2,*]

[1]Department of Chemistry, The University of Hong Kong, Hong Kong, China

[2]State Key Laboratory of Synthetic Chemistry, The University of Hong Kong, Hong Kong, China

*Correspondence: hoyuay@hku.hk

Keywords

catenane; co-conformational change; ion receptor; mechanical bond; mechano-stereochemistry

Abstract

Responsive synthetic receptors for adaptive recognition of different ionic guests in a competitive environment are valuable molecular tools for not only ion sensing and transport, but also the development of ion-responsive smart materials and related technologies. By virtue of the mechanical chelation and ability to undergo large-amplitude co-conformational changes, described herein is the discovery of a chameleon-like [2]catenane that selectively binds copper(I) or sulfate ions and its associated co-conformational mechanostereochemical switching. This work highlights not only the advantages and versatility of catenane as a molecular skeleton in receptor design, but also its potential in constructing complex responsive systems with multiple inputs and outputs.

Introduction

Selective recognition of ionic guests using synthetic molecular receptors has long attracted immense research interest for their significance and diverse applications in controlling ion transport in biological systems,[1–4] developing sensing and delivery agents for ionic species of environmental, diagnostic and therapeutic significance,[5–13] extracting and refining harmful and/or precious ionic components from waste and natural resources, etc.[14–17] Over the years, tremendous efforts have been devoted in the development of mono-, di- and multitopic molecular hosts for binding various ionic guests,[18–27] and recent studies have also been extended to responsive hosts featuring switchable ion binding ability.[28–32] In general, critical to a successful ion receptor is the precise spatial arrangement of the ion binding motifs within the receptor skeleton.[33,34] However, designing and synthesizing a highly complementary receptor

in terms of structure and surface interactions for a particular ionic guest are usually non-trivial, not to mention the engineering and control of additional mechanisms to achieve responsiveness and adaptability.

In contrast to constructing a fully complementary cavity by precisely positioning binding motifs within a rigid covalent backbone, partially relaxing the rigidity of the receptor skeleton may allow the host not only to optimize the host-guest interactions through conformational adjustment,[35–41] but also to respond and adapt to external stimuli and environmental changes. In this regard, catenanes and related mechanically interlocked molecules (MIMs), well-known for their ability to undergo co-conformational changes, are an attractive class of molecular framework for receptor design.[42–44] On one hand, binding motifs linked by mechanical bonds are still preorganized and the guest association will be strong due to mechanical chelation, and on the other hand, large-amplitude co-conformational rearrangement will be a facile and adaptive mechanism for optimizing the binding as well as responding to external changes.[45–49]

In this work, a heteroditopic [2]catenane containing both bipyridine (bpy) and urea motifs for respective cation and anion binding is described. In addition to copper(I) ion that templates its synthesis, the host also displays a strong and selective binding to sulfate anion (log $K_1 \sim 4.3$ and log $K_2 \sim 3.6$) in 5% aqueous DMSO, rendering the catenane as an unusual receptor featuring two structurally different mechanical chelates in the guest-bound forms. Contrary to the achiral copper(I)-bound and ion-free co-conformers, sulfate binding leads to a "180°-turn" of both macrocycles and stabilizes a chiral co-conformation of the [2]catenane.

Results and discussion

To efficiently obtain catenane-derived receptors, the Cu^+-templated, dynamic urea formation from building blocks **1** and **2** containing respectively *t*-butylamine and isocyanate functional groups was explored to simultaneously introduce both the cation binding bipyridine (bpy) and anion binding urea groups during the catenane synthesis.[50,51] Catenane **C** is obtained in four simple steps without any chromatographic purification (Figure 1). By virtue of the strong Cu^+-bpy template and the effective ring-closing from the "error-checking" dynamic urea formation, the catenane topology was efficiently created. Simple acid treatment removed the *t*-butyl group after the catenane formation, which locked the dynamic urea and activated their anion binding potential.[52] Catenane **C** was then obtained by using ethylenediamine to extract the Cu^+ template followed by aqueous washing.[53] For comparison, a control [2]catenane **C'** and macrocycle **M** featuring only one bis-urea bipyridine-based macrocycle were also prepared (Figure 1 and Scheme S1).

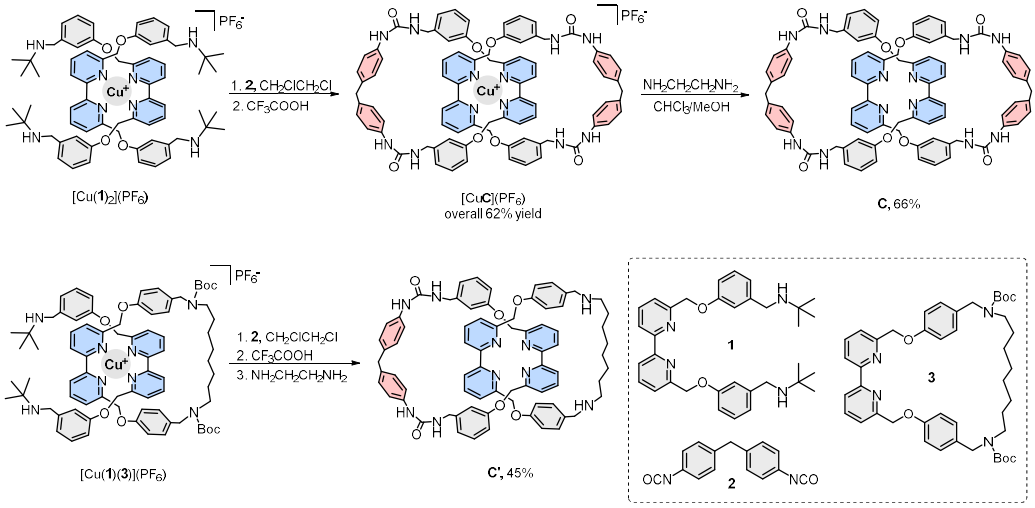

Figure 1. Synthesis of the tetra-urea catenane host **C** and the bis-urea control catenane **C'**.

HR-ESI-MS spectrum of **C** showed molecular ion peaks at *m/z* 1375.5458 [**C**+Na]$^+$ and 677.2873 [**C**+2H]$^{2+}$ that are consistent to the expected molecular formula $C_{82}H_{72}N_{12}O_8$ of the catenane, and the interlocked nature is evidenced by the direct fragmentation of the singly charged molecular ion peak to the constituting macrocycle at *m/z* 677.2837 [**M**+H]$^+$ in the MS/MS experiment (Figure S2). The ^{1}H NMR spectrum (600 MHz, 298 K, DMSO-d_6) of **C** showed that the catenane adopts a highly symmetrical structure with three H_{bpy} and two H_{dpm} resonances, suggesting that the two interlocked rings are equivalent and the [2]catenane possesses two C_2 axis. The two urea NH were found at 6.52 ppm and 8.25 ppm, which are similar to other reported urea-based macrocycles.[51,54] Only slight spectral changes were observed when the temperature was increased from 298 K to 358 K (Figure S20), which may be explained by a fast co-conformational exchange of the interlocked host.[55] Comparing the ^{1}H NMR spectra of **C** and the non-interlocked macrocycle **M**, proton resonances are generally more upfield shifted in the catenane due to a stronger shielding effect as a result of mechanical interlocking (e.g. $\Delta\delta$ ~ 0.52–0.61 ppm for H_{bpy} and 0.30–0.42 ppm for H_{dpm}).

Similar to most other metal-templated catenanes, the bis(bipyridine) cavity crafted in **C** as a legacy of the templated synthesis could be complementary for cation binding.[47,56–58] As expected, addition of [Cu(MeCN)$_4$](PF$_6$) to a solution of **C** led to the formation of a species with a new UV-Vis absorption at 450 nm characteristic to the Cu$^+$-to-bpy MLCT and a ^{1}H NMR spectrum consistent to that of [Cu**C**]$^+$ (Figures S24 and S26). The 1:1 Cu(I) complexation was found to be in slow exchange on the NMR timescale, and no further spectral changes were observed after one equivalent of Cu(I) ion had been administered. In the ^{1}H NMR spectrum of[Cu**C**](PF$_6$), resonances of the *meta*-substituted aryl spacer signals H_{Ar} are significantly

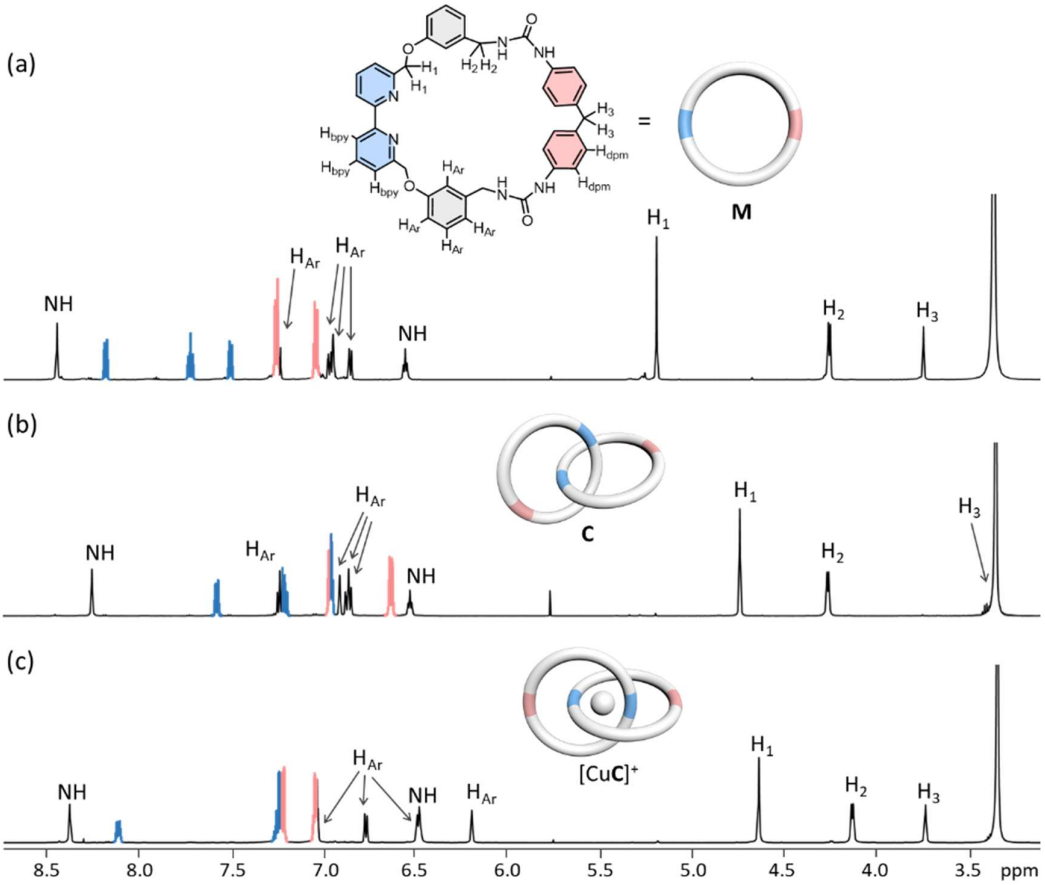

Figure 2. Partial ^{1}H NMR spectra (600 MHz, DMSO-d_6, 298 K) of (a) **M**, (b) **C** and (c) Cu(I) complex [Cu**C**](PF$_6$). Aromatic signals from bpy and dpm units are highlighted as blue and red respectively.

upfield shifted when compared to that of the free host (Figure 2), and NOE cross peaks between H_{Ar} and H_{bpy} were also found in the 2D NOESY spectrum (Figure S22). These spectral features are consistent with the reinforced π-stacking interactions between the aromatic units as a result of the Cu^{+}-bpy coordination.[50] Slight chemical shift changes were found for the urea NH, H_1 and H_2, and a more significant downfield shift by *ca.* 0.4 ppm was noticed for the diphenylmethylene (dpm) H_3. Because of the interlocked structure, the dpm linkers are likely perpendicularly oriented with respect to the bpy of the other macrocycles, hence placing H_3 in the deshielding region of the bpy in the Cu(I) complex.

While the Cu^{+} binding may not be surprising, the bpy-derived [2]catenane showed a very different cation selectivity than those closely related bis(phenanthroline) catenanes and MIMs, which also feature a preorganized cavity with four nitrogen coordination donors. Although catenanes with a bis(phenanthroline) core have been shown to form complexes with a range of

cations such as Li^+, Na^+, H^+, Ni^{2+}, Zn^{2+}, Cd^{2+} and Ag^+,[59,60] addition of Zn^{2+} or Na^+ ions to a DMSO solution of **C** resulted in no obvious change in the ^{1}H NMR and UV-Vis spectra (Figures S24 and S25). The strong preference of **C** towards Cu^+ may be ascribed to the flexibility of the bpy, in which bond rotation along the bpy axis could result in different orientations and coordination modes of the pyridines.[61–63] Yet, more extensive structural analysis and studies on the impact of catenand effect on the cation binding of bpy-based MIMs will be warranted to explain the observed cation selectivity.[64,65]

The incorporation of four hydrogen bonding urea motifs in the macrocycle backbone is envisaged to endow the [2]catenane **C** with potent anion binding capability. To investigate its anion recognition behavior, ^{1}H NMR anion titration experiments were conducted, in which aliquots of different anions (Cl^-, Br^-, I^-, NO_3^-, HSO_4^-, SO_4^{2-}, CH_3COO^-, $H_2PO_4^-$, PO_4^{3-}) as their tetrabutylammonium (TBA) salts were added to the catenane solutions in DMSO-d_6 (Figure S27). Only negligible spectral changes were observed when Br^-, I^-, NO_3^-, HSO_4^- were added, suggestive of no significant binding to these anions. In stark contrast, the addition of sulfate resulted in a drastic downfield perturbation to the urea NH signals ($\Delta\delta$ = 1.56 ppm and 2.22 ppm over 2 eq. of sulfate), suggesting the oxoanion is bound via the formation of urea NH hydrogen bonds (Figure 3). Further addition of sulfate (>2 eq.) did not induce further chemical shift changes, suggesting saturation of the urea anion binding sites. Downfield shifts of urea proton signals, in a less pronounced magnitude were also observed upon the addition of 10 eq. of Cl^-, $H_2PO_4^-$, PO_4^{3-} and CH_3COO^-, indicating that the catenane also binds to these anions but with a weaker affinity. The anion binding stoichiometry was revealed by Job plot (Figures S28 and S29), and the 1:1/1:2 host-guest anion association constants were determined from the titration data and are summarized in Table 1.

Table 1. Anion binding constants of catenane **C** and control compounds **C'** and **M**.[a]

	Anion binding of **C** in DMSO-d_6				
	SO_4^{2-}	AcO^-	$H_2PO_4^-$	PO_4^{3-}	Cl^-
K_1 (M^{-1})	$>10^5$	7700	3000	4800	160
K_2 (M^{-1})	$>10^5$	370	390	/	3
	Sulfate binding in 5% D_2O/DMSO-d_6				
	C		**C'**	**M**	
K_1 (M^{-1})	21000[b]		370	360	
K_2 (M^{-1})	3600		/	/	

[a] K_1 and K_2 values were calculated using Bindfit with 1:1 or 1:2 host-guest binding models.[66,67] Errors (±) are all <10% unless otherwise noted. All anions were added as TBA salts. [Host] = 1 or 2 mM. T = 298 K. [b] Error = 18.4%.

In particular, the catenane was found to be selective to sulfate with a 1:2 stoichiometry and binding constants of $>10^5$ M^{-1} in DMSO-d_6 for both the first and second sulfate association. Encouraged by the strong and selective binding of sulfate anion in DMSO-d_6, ^{1}H NMR titration experiment was carried out in the more competitive 5% D_2O in DMSO-d_6. For comparison, the sulfate association constants of the macrocycle **M**, and the control [2]catenane **C'** consisting of only one bis-urea-based bipyridine macrocycle, were also determined. Both macrocycle **M** and catenane **C'** displayed comparable 1:1 host-guest binding to sulfate anion with $K \sim 400$ M^{-1}. In contrast, the tetra-urea catenane **C** demonstrated significantly stronger 1:2 host-guest association to the oxoanion, with $K_1 = 2.1 \times 10^4$ M^{-1}, *ca.* 55-fold higher than those of macrocycle **M** and catenane **C'**. The sulfate complex can also be directly observed by HR-ESI-MS, in which peaks for the 1:1 and 1:2 sulfate complexes at *m/z* 1449.5154 [**C**+SO_4+H]$^+$, 1691.7937 [**C**+SO_4+TBA]$^+$ and 1789.7611 [**C**+2(SO_4)+2H+TBA]$^+$, with isotopic distributions corresponding to the respective molecular formula, were found in the MS spectrum (Figure 3). These findings suggest the mode of sulfate binding by **C** features a cooperative mechanical chelation of a sulfate anion by two urea groups from the two interlocked rings, and more importantly highlights the critical role of the mechanical flexibility for efficient, large-amplitude co-conformational rearrangement of the binding motifs despite of the rigidity of the covalent macrocyclic skeleton.

Apart from the strong binding in competitive aqueous environment, sulfate binding of **C** is also characterized by a distinctive structural change of the host. In addition to the hydrogen bonded urea NH, the ^{1}H NMR spectrum (500 MHz, DMSO-d_6, 298 K) of **C** in the presence of 10 eq. SO_4^{2-} also showed that the H_{bpy} resonances are downfield shifted to 8.34 ppm, 7.72 ppm and 7.58 ppm, while that of the H_{dpm} are more upfield at 6.69 ppm and 5.98 ppm when compared to that of the free host **C** and macrocycle **M**, suggestive of a respectively weaker and stronger shielding effect for the bpy and dpm units in the sulfate complex. Significant upfield shift of the dpm CH_2 (H_3) was also observed in the sulfate complex, indicating that **C** adopts a co-conformation in which the bpy are more exposed at the catenane exterior, and concomitantly the dpm are buried in the catenane center upon sulfate binding.[68] Compared to the co-conformation in [Cu**C**]$^+$ in which the bpy and dpm units locate respectively at the central and peripheral positions of the catenane, the two interlocked macrocycles have each undergone a "180°-turn", and the bpy and dpm "exchanged" their relative positions in the sulfate complex. Furthermore, the 2D NOESY spectrum of **C** obtained in the presence of 10 eq. SO_4^{2-} showed NOE cross peaks between H_{dpm} and H_{Ar} protons (Figure S23), which is consistent to the interlocked macrocycles rotated inside-out, such that the dpm units are now in a closer proximity to the *meta*-substituted aryl spacer of the other macrocycle. Noteworthily, literature examples of sulfate-selective receptors frequently invoke a hydrophobic effect from host

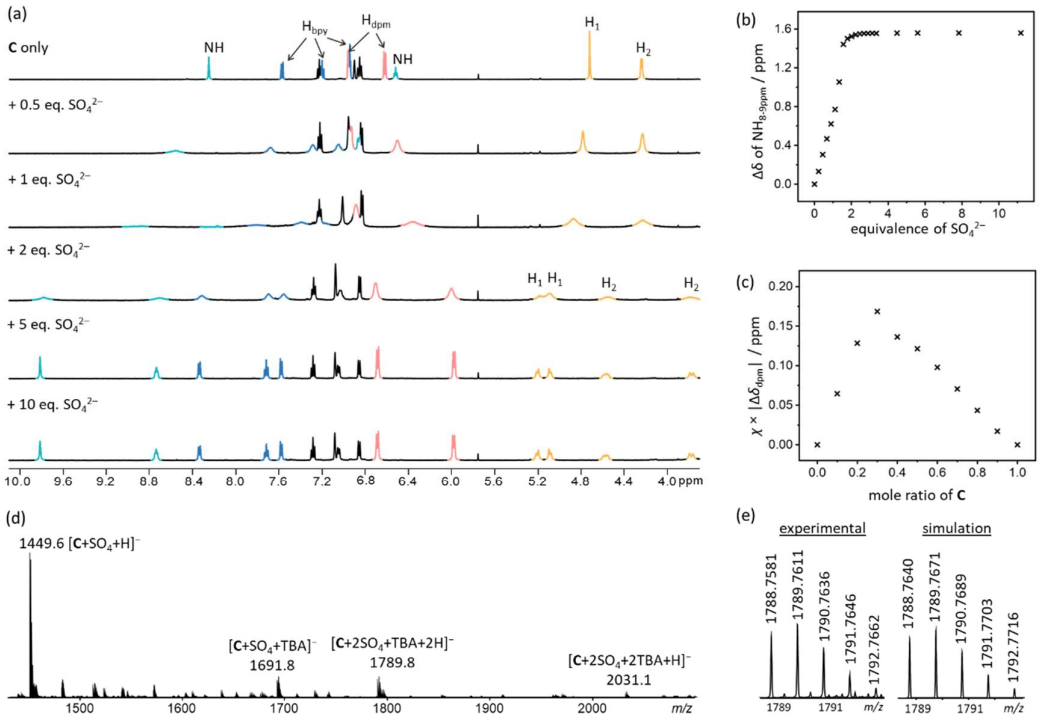

Figure 3. (a) Partial ^{1}H NMR (500 MHz, DMSO-d_6, 298 K) spectra of **C** in the presence of increasing amount of TBA sulfate. Methylene protons H_1 and H_2 become diastereotopic in the presence of 2 eq. or more of sulfate, (b) change in chemical shift of the urea NH proton originally at ~8.4 ppm, (c) Job plot of the binding showing a 1:2 host-guest stoichiometry, (d) HR-ESI-MS (-ve) spectrum obtained from a sample of **C** in the presence of 10 eq. of TBA sulfate, and (e) isotopic distribution of the mass signal at *m/z* 1789.8.

encapsulation of sulfate anions, which shields the highly hydrophilic anion and assists its desolvation in aqueous environment.[54,69–75] In contrast, sulfate anion induces a large-amplitude co-conformational change in the interlocked backbone of **C**, bringing the urea donors in the two macrocycles in proximity for convergent sulfate binding. The high flexibility and ability to undergo large-amplitude co-conformational change thus enable the catenane host to adapt to ionic guests of different size, charge, geometry and binding stoichiometry (i.e., 1:1 binding of monocationic, spherical Cu^+ and 1:2 binding of dianionic, tetrahedral SO_4^{2-}).

Sulfate binding also leads to a change in the stereochemistry of **C**. While the time-averaged structures of the free host and Cu(I) complex [Cu**C**]$^+$ display no chiral feature in our spectroscopic studies, diastereotopic splitting of the methylene singlets H_1 and H_2 to a pair of spin-coupled doublets can be observed in the presence of 10 eq. SO_4^{2-}, showing that the sulfate ions stabilize a specific chiral co-conformer of **C**. Weakening the sulfate association by adding D_2O to the NMR sample led to the coalescence of H_1 and H_2 doublets (Figure S38), and in the

presence of 5% D_2O (or more), the resulting ^1H NMR spectrum essentially showed no chiral feature although significant sulfate binding can still be measured as discussed previously. These findings not only confirm that sulfate selects and binds strongly to a chiral co-conformer of the catenane host, but also demonstrate a rare example in which the extent of chiral property expression can be controlled by the specific condition of host-guest binding. For both the Cu(I) and sulfate complexes of **C**, ^1H NMR analysis showed that the two interlocked macrocycles are equivalent, and both complexes are C_2 symmetric with respect to the catenane molecular axis with only three bpy and two dpm aromatic signals. Chirality of the sulfate complex is therefore explained by a "tilted" orientation of the two macrocyclic planes as a result of the rocking of the macrocycles being arrested by the sulfate binding, and such structure has been referred as being mechanically helically chiral (Figure 4).[76–83] On the other hand, the tetrahedral Cu^+-bpy coordination brings the bpy to the catenane center and enforces a perpendicular orientation of the macrocyclic planes to give an achiral structure. Other co-conformations of **C** are unlikely to be C_2 symmetric although some of them are also chiral.[84,85]

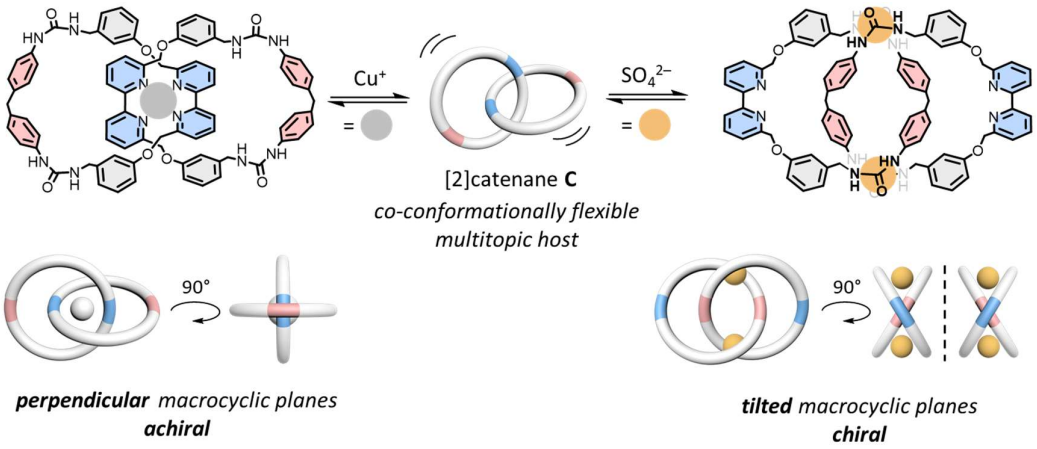

Figure 4. Co-conformational exchange of **C** involving a "180°-turn" of the macrocycles upon guest binding to produce achiral Cu(I) and chiral sulfate complexes.

Further structural details of the sulfate complex are revealed by single crystal X-ray diffraction analysis (Figure 5). Single crystals of the sulfate complex were obtained by slow vapor diffusion of diisopropyl ether into a DMF solution of **C** in the presence of 10 eq. TBA_2SO_4. The sulfate complex crystallized in the monoclinic $P2_1/n$ space group with each asymmetric unit consists of one catenane, one sulfate, two TBA ions and four DMF molecules. Consistent with the NMR structural studies, the catenane was found to adopt a co-conformation in which the dpm and bpy locate respectively in the catenane center and periphery, and an average

interplanar separation of 4.1 Å was found between the dpm units from the two macrocycles. The bpy units are also found to adopt a *trans* configuration that the two pyridine donors are pointing towards opposite directions, probably as a result of relieving any potential ring strain in the interlocked macrocycle. Eight N−H···O hydrogen bonds at a distance of 2.755–3.133 Å were identified between each of the sulfate and four urea groups from two different interlocked rings of two molecules of **C**, confirming the mechanical chelating mode of the sulfate binding. The chiral co-conformation is evidenced by the tilted arrangement of the macrocyclic planes at an angle of ~62°. The crystal sample is overall racemic and the enantiomeric co-conformers of opposite chirality are bridged by a sulfate ion in an alternate fashion to result in infinite 1D chains, which further align with adjacent strands at a distance of ~4.1 Å (Figure S42).

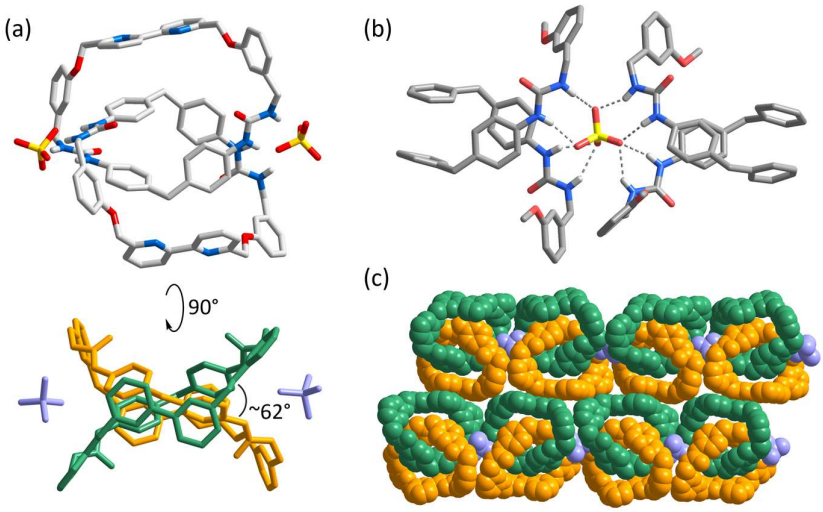

Figure 5. X-ray crystal structure showing (a) the sulfate catenane complex in different perspectives, (b) the hydrogen bonding interactions between the sulfate and urea groups from two catenanes and (c) arrangement of the enantiomeric co-conformers. TBA ions and DMF molecules are omitted for clarity.

The guest-controlled, reversible co-conformational mechanostereochemical switching of **C** was further demonstrated by the sequential introduction of Cu^{+} and SO_4^{2-}, as well as the competitive CN^{-} and Ba^{2+} ions. As shown in Figure 6, addition of 4 eq. of TBA_2SO_4 to a 1 mM DMSO-d_6 solution of **C** resulted in the formation of the 1:2 sulfate complex as shown by the downfield shifted urea NH, as well as the diastereotopic H_1 and H_2 resonances. This chiral, sulfate-bound form of **C** can be made co-conformationally flexible again by addition of $Ba(OTf)_2$ that led to the formation of $BaSO_4$ and reversed the spectral changes, with a resulting ^{1}H NMR spectrum essentially the same as that of the initial free host **C**. Further switching to the achiral form of

the Cu^+ complex was achieved by addition of $[Cu(MeCN)_4](PF_6)$, which produced a ^1H NMR spectrum with the H_{bpy} and H_{Ar} signals characteristic to a Cu^+-bis(bipyridine) in an overall achiral structure. The guest-free catenane was regenerated again by adding $[(Me_4N)(CN)]$ that competitively extracted the Cu^+ ion from the catenane, which could then switch on its sulfate binding ability and gave the chiral sulfate complex after the introduction of a second batch of TBA_2SO_4. The successful use of four ionic guests of different charges, geometry and properties to control a multitopic host to give two different stereochemical outcomes, by virtue of the exceptional co-conformational flexibility of the mechanical bond, hence highlights the unique potential of exploiting the topologically non-trivial catenane as a receptor skeleton in the design and development of diverse classes of smart and responsive molecular hosts.

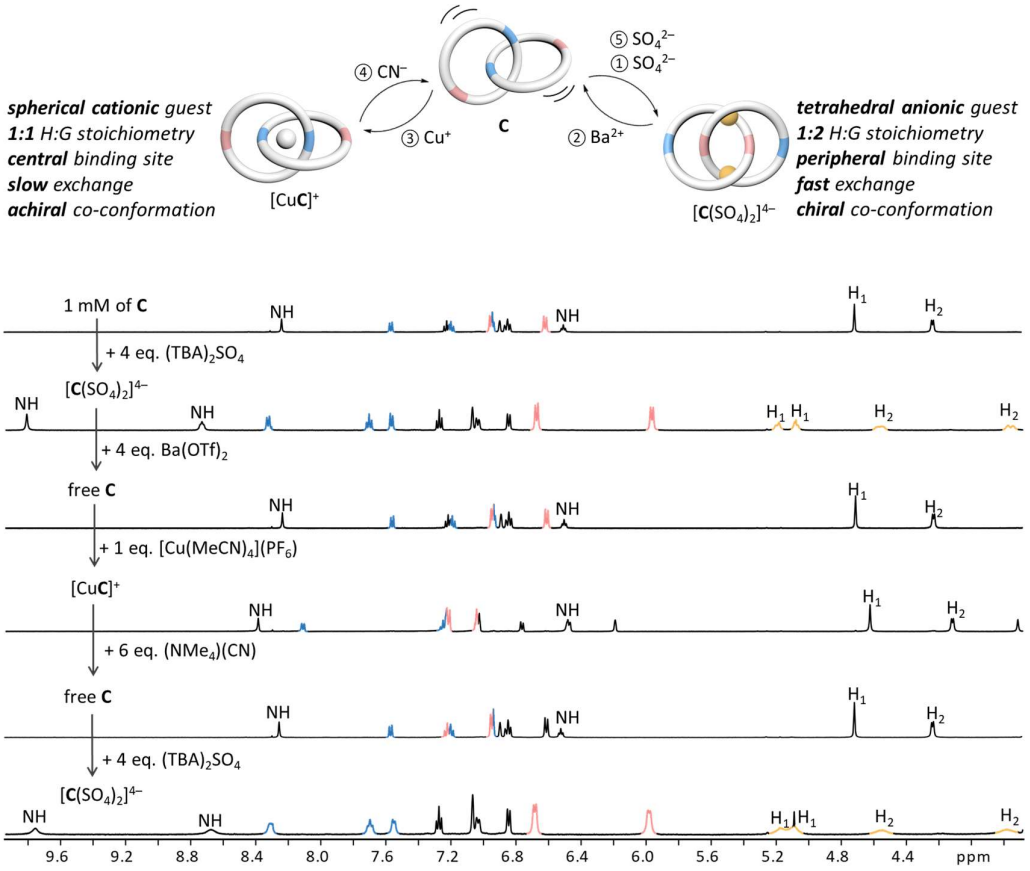

Figure 6. Reversible switching of **C** between achiral and chiral co-conformations by sequential addition of specific ionic guests.

Conclusion

In summary, a novel and efficient approach to prepare heteroditopic [2]catenane has been developed, exploiting the metal cation template-directed strategy and dynamic urea formation as ring-closing reaction. Extensive binding studies revealed that in addition to encapsulating the spherical Cu^{+} cation at the core via mechanical chelation of the two bipyridine ligands in an overall 1:1 stoichiometry, the [2]catenane is also capable of strong and selective binding to the tetrahedral SO_4^{2-} anion at the periphery mediated by urea hydrogen bonding formation in a 1:2 host-guest fashion. ^{1}H NMR analysis and X-ray crystallographic study showed the interlocked macrocycles are related by a "180°-circumrotation" in the Cu(I) and sulfate complexes, and saliently, whilst the former remains achiral, the catenane·sulfate complex is chiral with a tilted orientation of the macrocyclic planes. These findings not only highlight the advantages of using co-conformationally flexible catenane hosts for facile adaption and rearrangement of binding motifs to accommodate guests of various structural and electronic features, but also demonstrate a unique example in which the realms of dynamic mechanostereochemistry and host-guest chemistry characteristic to MIMs intersect, where new and unexplored opportunities may arise.

Acknowledgements

This work is supported by the CAS-Croucher Funding Scheme for Joint Laboratories and the Collaborative Research Fund (C7075-21G) from the Research Grants Councils of Hong Kong. Y. Y. is a recipient of the Postgraduate Scholarship from The University of Hong Kong. We acknowledge UGC funding administered by The University of Hong Kong for support of the Electrospray Ionisation Quadrupole Time-of-Flight Mass Spectrometry Facilities under the support for Interdisciplinary Research in Chemical Science.

Author contributions

Y. Yao: Conceptualization, Methodology, Formal Analysis, Investigation, Writing – Original Draft, Visualization; Y. C. Tse: Methodology, Formal Analysis, Writing – Review & Editing; S. K.-M. Lai: Investigation; Y. Shi: Formal Analysis, Visualization; K.-H. Low: Investigation; H. Y. Au-Yeung: Conceptualization, Formal Analysis, Writing – Original Draft, Writing – Review & Editing, Visualization, Supervision, Project administration, Funding acquisition.

Declaration of interests

The authors declare no competing interests.

References

1. Matile, S., Vargas Jentzsch, A., Montenegro, J., and Fin, A. (2011). Recent synthetic transport systems. Chem. Soc. Rev. *40*, 2453–2474. https://doi.org/10.1039/C0CS00209G.
2. Gale, P.A. (2011). From anion receptors to transporters. Acc. Chem. Res. *44*, 216–226. https://doi.org/10.1021/ar100134p.
3. Gale, P.A., Pérez-Tomás, R., and Quesada, R. (2013). Anion transporters and biological systems. Acc. Chem. Res. *46*, 2801–2813. https://doi.org/10.1021/ar400019p.
4. Mondal, A., Ahmad, M., Mondal, D., and Talukdar, P. (2023). Progress and prospects toward supramolecular bioactive ion transporters. Chem. Commun. *59*, 1917–1938. https://doi.org/10.1039/D2CC06761G.
5. Beer, P.D., and Gale, P.A. (2001). Anion recognition and sensing: the state of the art and future perspectives. Angew. Chem. Int. Ed. *40*, 486–516. https://doi.org/10.1002/1521-3773(20010202)40:3<486::AID-ANIE486>3.0.CO;2-P.
6. Domaille, D.W., Que, E.L., and Chang, C.J. (2008). Synthetic fluorescent sensors for studying the cell biology of metals. Nat. Chem. Biol. *4*, 168–175. https://doi.org/10.1038/nchembio.69.
7. Teresa Albelda, M., Frías, J.C., García-España, E., and Schneider, H.-J. (2012). Supramolecular complexation for environmental control. Chem. Soc. Rev. *41*, 3859–3877. https://doi.org/10.1039/C2CS35008D.
8. Yeung, M.C.-L., and Yam, V.W.-W. (2015). Luminescent cation sensors: from host–guest chemistry, supramolecular chemistry to reaction-based mechanisms. Chem. Soc. Rev. *44*, 4192–4202. https://doi.org/10.1039/C4CS00391H.
9. Gale, P.A., and Caltagirone, C. (2015). Anion sensing by small molecules and molecular ensembles. Chem. Soc. Rev. *44*, 4212–4227. https://doi.org/10.1039/C4CS00179F.
10. Katayev, E.A., Kolesnikov, G. V, and Sessler, J.L. (2009). Molecular recognition of pertechnetate and perrhenate. Chem. Soc. Rev. *38*, 1572–1586. https://doi.org/10.1039/B806468G.
11. Heffern, M.C., Matosziuk, L.M., and Meade, T.J. (2014). Lanthanide probes for bioresponsive imaging. Chem. Rev. *114*, 4496–4539. https://doi.org/10.1021/cr400477t.
12. Gale, P.A., Davis, J.T., and Quesada, R. (2017). Anion transport and supramolecular medicinal chemistry. Chem. Soc. Rev. *46*, 2497–2519. https://doi.org/10.1039/C7CS00159B.
13. Yang, J., Yu, G., Sessler, J.L., Shin, I., Gale, P.A., and Huang, F. (2021). Artificial transmembrane ion transporters as potential therapeutics. Chem *7*, 3256–3291. https://doi.org/10.1016/j.chempr.2021.10.028.
14. Hargrove, A.E., Nieto, S., Zhang, T., Sessler, J.L., and Anslyn, E. V (2011). Artificial receptors for the recognition of phosphorylated molecules. Chem. Rev. *111*, 6603–6782. https://doi.org/10.1021/cr100242s.
15. Liu, Z., Frasconi, M., Lei, J., Brown, Z.J., Zhu, Z., Cao, D., Iehl, J., Liu, G., Fahrenbach, A.C., Botros, Y.Y., et al. (2013). Selective isolation of gold facilitated by second-sphere coordination with α-cyclodextrin. Nat. Commun. *4*, 1855. https://doi.org/10.1038/ncomms2891.
16. Banerjee, D., Kim, D., Schweiger, M.J., Kruger, A.A., and Thallapally, P.K. (2016). Removal of TcO_4^- ions from solution: materials and future outlook. Chem. Soc. Rev. *45*, 2724–2739. https://doi.org/10.1039/C5CS00330J.

17. Williams, G.T., Haynes, C.J.E., Fares, M., Caltagirone, C., Hiscock, J.R., and Gale, P.A. (2021). Advances in applied supramolecular technologies. Chem. Soc. Rev. *50*, 2737–2763. https://doi.org/10.1039/D0CS00948B.
18. Christensen, J.J., Eatough, D.J., and Izatt, R.M. (1974). The synthesis and ion bindings of synthetic multidentate macrocyclic compounds. Chem. Rev. *74*, 351–384. https://doi.org/10.1021/cr60289a003.
19. Liu, Z., Nalluri, S.K.M., and Stoddart, J.F. (2017). Surveying macrocyclic chemistry: from flexible crown ethers to rigid cyclophanes. Chem. Soc. Rev. *46*, 2459–2478. https://doi.org/10.1039/C7CS00185A.
20. Katayev, E.A., Ustynyuk, Y.A., and Sessler, J.L. (2006). Receptors for tetrahedral oxyanions. Coord. Chem. Rev. *250*, 3004–3037. https://doi.org/10.1016/j.ccr.2006.04.013.
21. Kubik, S. (2009). Amino acid containing anion receptors. Chem. Soc. Rev. *38*, 585–605. https://doi.org/10.1039/B810531F.
22. Kang, S.O., Llinares, J.M., Day, V.W., and Bowman-James, K. (2010). Cryptand-like anion receptors. Chem. Soc. Rev. *39*, 3980–4003. https://doi.org/10.1039/C0CS00083C.
23. Evans, N.H., and Beer, P.D. (2014). Advances in anion supramolecular chemistry: from recognition to chemical applications. Angew. Chem. Int. Ed. *53*, 11716–11754. https://doi.org/10.1002/anie.201309937.
24. Macreadie, L.K., Gilchrist, A.M., McNaughton, D.A., Ryder, W.G., Fares, M., and Gale, P.A. (2022). Progress in anion receptor chemistry. Chem *8*, 46–118. https://doi.org/10.1016/j.chempr.2021.10.029.
25. Kim, S.K., and Sessler, J.L. (2010). Ion pair receptors. Chem. Soc. Rev. *39*, 3784–3809. https://doi.org/10.1039/C002694H.
26. McConnell, A.J., and Beer, P.D. (2012). Heteroditopic receptors for ion-pair recognition. Angew. Chem. Int. Ed. *51*, 5052–5061. https://doi.org/10.1002/anie.201107244.
27. He, Q., Vargas-Zúñiga, G.I., Kim, S.H., Kim, S.K., and Sessler, J.L. (2019). Macrocycles as ion pair receptors. Chem. Rev. *119*, 9753–9835. https://doi.org/10.1021/acs.chemrev.8b00734.
28. Busschaert, N., Elmes, R.B.P., Czech, D.D., Wu, X., Kirby, I.L., Peck, E.M., Hendzel, K.D., Shaw, S.K., Chan, B., Smith, B.D., et al. (2014). Thiosquaramides: pH switchable anion transporters. Chem. Sci. *5*, 3617–3626. https://doi.org/10.1039/C4SC01629G.
29. Qu, D.-H., Wang, Q.-C., Zhang, Q.-W., Ma, X., and Tian, H. (2015). Photoresponsive host–guest functional systems. Chem. Rev. *115*, 7543–7588. https://doi.org/10.1021/cr5006342.
30. Sahoo, P.R., Prakash, K., and Kumar, S. (2018). Light controlled receptors for heavy metal ions. Coord. Chem. Rev. *357*, 18–49. https://doi.org/10.1016/j.ccr.2017.11.010.
31. Fares, M., Wu, X., Ramesh, D., Lewis, W., Keller, P.A., Howe, E.N.W., Pérez-Tomás, R., and Gale, P.A. (2020). Stimuli-responsive cycloaurated "OFF-ON" switchable anion transporters. Angew. Chem. Int. Ed. *59*, 17614–17621. https://doi.org/10.1002/anie.202006392.
32. Wezenberg, S.J. (2022). Photoswitchable molecular tweezers: isomerization to control substrate binding, and what about vice versa? Chem. Commun. *58*, 11045–11058. https://doi.org/10.1039/d2cc04329g.
33. Hay, B.P., Firman, T.K., and Moyer, B.A. (2005). Structural design criteria for anion hosts: strategies for achieving anion shape recognition through the complementary placement of urea donor groups. J. Am. Chem. Soc. *127*, 1810–1819. https://doi.org/10.1021/ja043995k.

34. Amendola, V., Bonizzoni, M., Esteban-Gómez, D., Fabbrizzi, L., Licchelli, M., Sancenón, F., and Taglietti, A. (2006). Some guidelines for the design of anion receptors. Coord. Chem. Rev. *250*, 1451–1470. https://doi.org/10.1016/j.ccr.2006.01.006.
35. Sanders, J.K.M. (1998). Supramolecular catalysis in transition. Chem. Eur. J. *4*, 1378–1383. https://doi.org/10.1002/(SICI)1521-3765(19980807)4:8<1378::AID-CHEM1378>3.0.CO;2-3.
36. Robertson, A., and Shinkai, S. (2000). Cooperative binding in selective sensors, catalysts and actuators. Coord. Chem. Rev. *205*, 157–199. https://doi.org/10.1016/S0010-8545(00)00243-5.
37. Badjić, J.D., Nelson, A., Cantrill, S.J., Turnbull, W.B., and Stoddart, J.F. (2005). Multivalency and cooperativity in supramolecular chemistry. Acc. Chem. Res. *38*, 723–732. https://doi.org/10.1021/ar040223k.
38. Hunter, C.A., and Anderson, H.L. (2009). What is cooperativity? Angew. Chem. Int. Ed. *48*, 7488–7499. https://doi.org/10.1002/anie.200902490.
39. Au-Yeung, H.Y., Cougnon, F.B.L., Otto, S., Pantoş, G.D., and Sanders, J.K.M. (2010). Exploiting donor–acceptor interactions in aqueous dynamic combinatorial libraries: exploratory studies of simple systems. Chem. Sci. *1*, 567–574. https://doi.org/10.1039/C0SC00307G.
40. Beeren, S.R., and Sanders, J.K.M. (2011). Discovery of linear receptors for multiple dihydrogen phosphate ions using dynamic combinatorial chemistry. J. Am. Chem. Soc. *133*, 3804–3807. https://doi.org/10.1021/ja200130h.
41. von Krbek, L.K.S., Schalley, C.A., and Thordarson, P. (2017). Assessing cooperativity in supramolecular systems. Chem. Soc. Rev. *46*, 2622–2637. https://doi.org/10.1039/C7CS00063D.
42. Gil-Ramírez, G., Leigh, D.A., and Stephens, A.J. (2015). Catenanes: fifty years of molecular links. Angew. Chem. Int. Ed. *54*, 6110–6150. https://doi.org/10.1002/anie.201411619.
43. Bruns, C. J. and Stoddart, J. F. (2016). The Nature of the Mechanical Bond: From Molecules to Machines (Wiley).
44. Au-Yeung, H.Y., and Deng, Y. (2022). Distinctive features and challenges in catenane chemistry. Chem. Sci. *13*, 3315–3334. https://doi.org/10.1039/D1SC05391D.
45. Langton, M.J., and Beer, P.D. (2014). Rotaxane and catenane host structures for sensing charged guest species. Acc. Chem. Res. *47*, 1935–1949. https://doi.org/10.1021/ar500012a.
46. Denis, M., Qin, L., Turner, P., Jolliffe, K.A., and Goldup, S.M. (2018). A fluorescent ditopic rotaxane ion-pair host. Angew. Chem. Int. Ed. *57*, 5315–5319. https://doi.org/10.1002/anie.201713105.
47. Inthasot, A., Tung, S.-T., and Chiu, S.-H. (2018). Using alkali metal ions to template the synthesis of interlocked molecules. Acc. Chem. Res. *51*, 1324–1337. https://doi.org/10.1021/acs.accounts.8b00071.
48. Bąk, K.M., Porfyrakis, K., Davis, J.J., and Beer, P.D. (2020). Exploiting the mechanical bond for molecular recognition and sensing of charged species. Mater. Chem. Front. *4*, 1052–1073. https://doi.org/10.1039/C9QM00698B.
49. Tay, H.M., Tse, Y.C., Docker, A., Gateley, C., Thompson, A.L., Kuhn, H., Zhang, Z., and Beer, P.D. (2023). Halogen-bonding heteroditopic [2]catenanes for recognition of alkali metal/halide ion pairs. Angew. Chem. Int. Ed. *62*, e202214785. https://doi.org/10.1002/anie.202214785.

50. Price, J.R., Clegg, J.K., Fenton, R.R., Lindoy, L.F., McMurtrie, J.C., Meehan, G. V, Parkin, A., Perkins, D., and Turner, P. (2009). Copper(I) templated synthesis of a 2,2-bipyridine derived 2-catenane: synthetic, modelling, and X-ray studies. Aust. J. Chem. *62*, 1014–1019. https://doi.org/10.1071/CH09253.
51. Yang, Y., Ying, H., Li, Z., Wang, J., Chen, Y., Luo, B., Gray, D.L., Ferguson, A., Chen, Q., Z, Y., et al. (2021). Near quantitative synthesis of urea macrocycles enabled by bulky *N*-substituent. Nat. Commun. *12*, 1572. https://doi.org/10.1038/s41467-021-21678-3.
52. Yang, Y., Ying, H., Jia, Y., Chen, Y., and Cheng, J. (2021). Stabilization of the hindered urea bond through de-tert-butylation. Chem. Commun. *57*, 3812–3815. https://doi.org/10.1039/d1cc00715g.
53. Yao, Y., Deng, Y., Kong, L., and Au-Yeung, H.Y. (2022). Efficient copper(I) extraction by ethylenediamine from stable catenane complexes. Eur. J. Inorg. Chem. *2022*, e202200271. https://doi.org/10.1002/ejic.202200271.
54. Kaur, S., Day, V.W., and Bowman-James, K. (2020). Urea-based macrocycle selective for sulfate and structurally sensitive to water. Cryst. Growth Des. *20*, 4212–4216. https://doi.org/10.1021/acs.cgd.0c00411.
55. Attempt to obtain the low-temperature NMR spectrum of **C** in other solvents such as $CDCl_3$ failed due to its poor solubility.
56. Crowley, J.D., Goldup, S.M., Lee, A.-L., Leigh, D.A., and McBurney, R.T. (2009). Active metal template synthesis of rotaxanes, catenanes and molecular shuttles. Chem. Soc. Rev. *38*, 1530–1541. https://doi.org/10.1039/B804243H.
57. Beves, J.E., Blight, B.A., Campbell, C.J., Leigh, D.A., and McBurney, R.T. (2011). Strategies and tactics for the metal-directed synthesis of rotaxanes, knots, catenanes, and higher order links. Angew. Chem. Int. Ed. *50*, 9260–9327. https://doi.org/10.1002/anie.201007963.
58. Lewis, J.E.M., Beer, P.D., Loeb, S.J., and Goldup, S.M. (2017). Metal ions in the synthesis of interlocked molecules and materials. Chem. Soc. Rev. *46*, 2577–2591. https://doi.org/10.1039/C7CS00199A.
59. Cesario, M., Dietrich, C.O., Edel, A., Guilhem, J., Kintzinger, J.P., Pascard, C., and Sauvage, J.P. (1986). Topological enhancement of basicity: molecular structure and solution study of a monoprotonated catenand. J. Am. Chem. Soc. *108*, 6250–6254. https://doi.org/10.1021/ja00280a023.
60. Armaroli, N., De Cola, L., Balzani, V., Sauvage, J.-P., Dietrich-Buchecker, C.O., Kern, J.-M., and Bailal, A. (1993). Absorption and emission properties of a 2-catenand, its protonated forms, and its complexes with Li^+, Cu^+, Ag^+, Co^{2+}, Ni^{2+}, Zn^{2+}, Pd^{2+} and Cd^{2+}: tuning of the luminescence over the whole visible spectral region. J. Chem. Soc., Dalt. Trans. 3241–3247. https://doi.org/10.1039/DT9930003241.
61. Kaes, C., Katz, A., and Hosseini, M.W. (2000). Bipyridine: the most widely used ligand. A review of molecules comprising at least two 2,2'-bipyridine units. Chem. Rev. *100*, 3553–3590. https://doi.org/10.1021/cr990376z.
62. Ziessel, R. (2001). Schiff-based bipyridine ligands. Unusual coordination features and mesomorphic behaviour. Coord. Chem. Rev. *216–217*, 195–223. https://doi.org/10.1016/S0010-8545(00)00410-0.
63. Hazell, A. (2004). Is bipyridine planar in metal complexes? Polyhedron *23*, 2081–2083. https://doi.org/10.1016/j.poly.2004.06.001.
64. Albrecht-Gary, A.M., Saad, Z., Dietrich-Buchecker, C.O., and Sauvage, J.P. (1985). Interlocked macrocyclic ligands: a kinetic catenand effect in copper(I) complexes. J. Am. Chem. Soc. *107*, 3205–3209. https://doi.org/10.1021/ja00297a028.

65. Cirulli, M., Kaur, A., Lewis, J.E.M., Zhang, Z., Kitchen, J.A., Goldup, S.M., and Roessler, M.M. (2019). Rotaxane-based transition metal complexes: effect of the mechanical bond on structure and electronic properties. J. Am. Chem. Soc. *141*, 879–889. https://doi.org/10.1021/jacs.8b09715.
66. Bindfit. http://app.supramolecular.org/bindfit/.
67. Thordarson, P. (2011). Determining association constants from titration experiments in supramolecular chemistry. Chem. Soc. Rev. *40*, 1305–1323. https://doi.org/10.1039/C0CS00062K.
68. Au-Yeung, H.Y., Pantoş, G.D., and Sanders, J.K.M. (2010). A water soluble donor–acceptor [2]catenane that can switch between a coplanar and a gemini-sign conformation. Angew. Chem. Int. Ed. *49*, 5331–5334. https://doi.org/10.1002/anie.201000807.
69. Kubik, S., Kirchner, R., Nolting, D., and Seidel, J. (2002). A molecular oyster: a neutral anion receptor containing two cyclopeptide subunits with a remarkable sulfate affinity in aqueous solution. J. Am. Chem. Soc. *124*, 12752–12760. https://doi.org/10.1021/ja026996q.
70. Otto, S., and Kubik, S. (2003). Dynamic combinatorial optimization of a neutral receptor that binds inorganic anions in aqueous solution. J. Am. Chem. Soc. *125*, 7804–7805. https://doi.org/10.1021/ja0351589.
71. Bondy, C.R., Gale, P.A., and Loeb, S.J. (2004). Metal−organic anion receptors: arranging urea hydrogen-bond donors to encapsulate sulfate ions. J. Am. Chem. Soc. *126*, 5030–5031. https://doi.org/10.1021/ja039712q.
72. Fowler, C.J., Haverlock, T.J., Moyer, B.A., Shriver, J.A., Gross, D.E., Marquez, M., Sessler, J.L., Hossain, M.A., and Bowman-James, K. (2008). Enhanced anion exchange for selective sulfate extraction: overcoming the Hofmeister bias. J. Am. Chem. Soc. *130*, 14386–14387. https://doi.org/10.1021/ja806511b.
73. Zhou, H., Zhao, Y., Gao, G., Li, S., Lan, J., and You, J. (2013). Highly selective fluorescent recognition of sulfate in water by two rigid tetrakisimidazolium macrocycles with peripheral chains. J. Am. Chem. Soc. *135*, 14908–14911. https://doi.org/10.1021/ja406638b.
74. Jia, C., Wang, Q.-Q., Begum, R.A., Day, V.W., and Bowman-James, K. (2015). Chelate effects in sulfate binding by amide/urea-based ligands. Org. Biomol. Chem. *13*, 6953–6957. https://doi.org/10.1039/C5OB00618J.
75. Kundu, S., Egboluche, T.K., and Hossain, M.A. (2023). Urea- and thiourea-based receptors for anion binding. Acc. Chem. Res. https://doi.org/10.1021/acs.accounts.2c00701.
76. Jamieson, E.M.G., Modicom, F., and Goldup, S.M. (2018). Chirality in rotaxanes and catenanes. Chem. Soc. Rev. *47*, 5266–5311. https://doi.org/10.1039/C8CS00097B.
77. Dietrich-Buchecker, C.O., Edel, A., Kintzinger, J.P., and Sauvage, J.P. (1987). Synthese et etude d'un catenate de cuivre chiral comportant deux anneaux coordinant a 27 atomes. Tetrahedron *43*, 333–344. https://doi.org/10.1016/S0040-4020(01)89961-0.
78. Tseng, H.-R., Vignon, S.A., Celestre, P.C., Stoddart, J.F., White, A.J.P., and Williams, D.J. (2003). Dynamic chirality: keen selection in the face of stereochemical diversity in mechanically bonded compounds. Chem. Eur. J. *9*, 543–556. https://doi.org/10.1002/chem.200390057.
79. Vignon, S.A., Wong, J., Tseng, H.-R., and Stoddart, J.F. (2004). Helical chirality in donor-acceptor catenanes. Org. Lett. *6*, 1095–1098. https://doi.org/10.1021/ol0364881.
80. Hori, A., Akasaka, A., Biradha, K., Sakamoto, S., Yamaguchi, K., and Fujita, M. (2002). Chirality induction through the reversible catenation of coordination rings. Angew.

Chem. Int. Ed. *41*, 3269–3272. https://doi.org/10.1002/1521-3773(20020902)41:17<3269::AID-ANIE3269>3.0.CO;2-9.

81. Nakatani, Y., Furusho, Y., and Yashima, E. (2010). Amidinium carboxylate salt bridges as a recognition motif for mechanically interlocked molecules: synthesis of an optically active [2]catenane and control of its structure. Angew. Chem. Int. Ed. *49*, 5463–5467. https://doi.org/10.1002/anie.201002382.
82. Prakasam, T., Lusi, M., Nauha, E., Olsen, J.-C., Sy, M., Platas-Iglesias, C., Charbonnière, L.J., and Trabolsi, A. (2015). Dynamic stereoisomerization in inherently chiral bimetallic [2]catenanes. Chem. Commun. *51*, 5840–5843. https://doi.org/10.1039/C4CC07392D.
83. Gidron, O., Jirásek, M., Trapp, N., Ebert, M.-O., Zhang, X., and Diederich, F. (2015). Homochiral [2]catenane and bis[2]catenane from alleno-acetylenic helicates - a highly selective narcissistic self-sorting process. J. Am. Chem. Soc. *137*, 12502–12505. https://doi.org/10.1021/jacs.5b08649.
84. Caprice, K., Pál, D., Besnard, C., Galmés, B., Frontera, A., and Cougnon, F.B.L. (2021). Diastereoselective amplification of a mechanically chiral [2]catenane. J. Am. Chem. Soc. *143*, 11957–11962. https://doi.org/10.1021/jacs.1c06557.
85. Rodríguez-Rubio, A., Savoini, A., Modicom, F., Butler, P., and Goldup, S.M. (2022). A co-conformationally “topologically” chiral catenane. J. Am. Chem. Soc. *144*, 11927–11932. https://doi.org/10.1021/jacs.2c02029.